NASA TECHNICAL NOTE

NASA TN D-4772

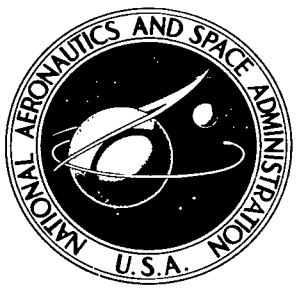

ON THE PREDICTION OF THE VIBRATORY BEHAVIOR OF FREE-FREE TRUNCATED CONICAL SHELLS

by Eugene C. Naumann

Langley Research Center
Langley Station, Hampton, Va.

NATIONAL AERONAUTICS AND SPACE ADMINISTRATION • WASHINGTON, D. C. • SEPTEMBER 1968

ON THE PREDICTION OF THE VIBRATORY BEHAVIOR OF FREE-FREE TRUNCATED CONICAL SHELLS

By Eugene C. Naumann

Langley Research Center
Langley Station, Hampton, Va.

NATIONAL AERONAUTICS AND SPACE ADMINISTRATION

For sale by the Clearinghouse for Federal Scientific and Technical Information
Springfield, Virginia 22151 – CFSTI price $3.00

ON THE PREDICTION OF THE VIBRATORY BEHAVIOR OF FREE-FREE TRUNCATED CONICAL SHELLS

By Eugene C. Naumann
Langley Research Center

SUMMARY

An analytical procedure is described for the prediction of the frequencies and mode shapes for free-free truncated conical shells. The method utilizes simple power series modal assumptions in a Rayleigh-Ritz type solution procedure. Excellent agreement was obtained when analytical results were compared with experimentally obtained frequencies and meridional mode shapes. Comparisons between analytical and experimental results are presented for truncated conical shells over the following range of parameters: (1) semivertex angles from 3.4° to 60.5°, (2) shell thicknesses from 0.0178 cm to 0.0813 cm, (3) shell truncation ratio (minimum radius/maximum radius) from 1/8 to 6/7, (4) shell maximum radius from 15.43 cm to 60.96 cm, and (5) materials – aluminum alloy, cold rolled steel, and stainless steel.

INTRODUCTION

The requirement for high-drag—low-weight vehicles for entry into rarified planetary atmospheres has resulted in exploration of the advantages of large-area—thin-skin decelerators. A typical structure of this type is the proposed 120° truncated cone Mars entry vehicle. These large thin-skin conical decelerators, inherently possess vibration characteristics that can be undesirable, difficult to attenuate satisfactorily, and, with current analytical procedures, difficult to predict. Experimental vibration data, from truncated conical shells tested with free-free end conditions, found in the literature provide data for a wide range of truncated cone configurations. Previous analytical methods for predicting the frequencies and mode shapes for free-free truncated conical shells include empirical (e.g., ref. 1), approximate inextensional (e.g., ref. 2), and modified Galerkin (e.g., ref. 3). Each of the methods is limited, in general, to the small range of vibrations associated with the lowest meridional mode.

An approach for predicting the free-free vibrational characteristics over a wider range of model geometries and circumferential and meridional mode combinations is needed. Accordingly, an analytical investigation has been carried out to develop a procedure utilizing a Rayleigh-Ritz type solution technique. Simple power series with

arbitrary coefficients and trigonometric functions are used for assumed meridional and circumferential mode shapes, respectively. In addition, the analytical procedure has been used to determine frequencies and mode shapes for several conical models for which data were found in the literature. The analytical procedure developed is presented herein together with comparisons between analytical and experimental frequencies, as well as mode shape data where possible.

SYMBOLS

Any consistent system of units may be used in this analysis.

C	shell extensional stiffness, $\frac{Eh}{1 - \mu^2}$
D	shell bending stiffness, $\frac{Eh^3}{12(1 - \mu^2)}$
E	shell modulus of elasticity
h	shell thickness
m	meridional mode number
n	circumferential mode number
r	radius of middle surface of shell
s	meridional coordinate of shell middle surface
t	time
T	kinetic energy
u	meridional displacement
U	strain energy
v	circumferential displacement

w	normal displacement
ϕ	circumferential coordinate of shell middle surface
$\alpha,\beta,\gamma,\theta,\psi,$ $\lambda,\epsilon,\eta,\kappa$	matrix elements in frequency equation
ω	frequency parameter
δ	semivertex angle
μ	Poisson's ratio
ρ	shell mass density
a,b,c, d,e,f	arbitrary coefficients in mode shapes

Subscripts:

j,k	identify modal components
1,2	refer to values at shell minimum and maximum radii, respectively
,s;,ϕ;,t	denote partial differentiation with respect to that variable

ANALYTICAL INVESTIGATION

The analytical investigation reported herein is a linear analysis, employing the Rayleigh-Ritz method, of a truncated conical shell with free-free edge conditions. The Rayleigh-Ritz method requires that the assumed modes satisfy the geometric restraints (i.e., for free-free boundary conditions the inplane and normal shell middle surface displacements and slopes do not vanish at the free edges) but does not require that the assumed modes satisfy the force restraints (i.e., moments and shears equal to zero at the free edges).

The coordinate system, illustrated in figure 1, has its origin at the imaginary apex of the shell with the Z-axis of the coordinate system, coincident with the shell axis of symmetry. The radius r to the shell middle surface is taken normal to the Z-axis and is related to the shell middle surface slant length s by the expression $r = s \sin \delta$,

where δ is the shell semivertex angle. The circumferential coordinate ϕ is the angle formed by the radius and the X-axis. The location of the X-axis on the shell is arbitrary because the shell is a symmetric body of revolution. The orthogonal inplane and normal shell middle surface displacements u, v, and w are assigned directions as follows: inplane meridional displacement, u positive along and coincident with the slant length s; inplane circumferential displacement, v positive with increasing ϕ; and normal displacement, w positive outward.

Method of Analysis

Strain and kinetic energy.- The linear strain-displacement relations of Novozhilov (ref. 4, ch. 1) were used to write the strain energy of a thin truncated conical shell (fig. 1), hereinafter called conical shell, in the following form:

$$U = \frac{C}{2}\int_0^{2\pi}\int_{s_1}^{s_2}\left[u_{,s}^2 + \left(\frac{1}{s}u + \frac{1}{s\sin\delta}v_{,\phi} + \frac{\cos\delta}{s\sin\delta}w\right)^2 + 2\mu\left(u_{,s}\right)\left(\frac{1}{s}u + \frac{1}{s\sin\delta}v_{,\phi}\right.\right.$$

$$\left.\left. + \frac{\cos\delta}{s\sin\delta}w\right) + \frac{1-\mu}{2}\left(\frac{1}{s\sin\delta}u_{,\phi} - \frac{v}{s} + v_{,s}\right)^2\right]s\sin\delta\,ds\,d\phi + \frac{D}{2}\int_0^{2\pi}\int_{s_1}^{s_2}\left[-w_{,ss}^2\right.$$

$$+ \left(\frac{\cos\delta}{s^2\sin^2\delta}v_{,\phi} - \frac{1}{s}w_{,s} - \frac{1}{s^2\sin^2\delta}w_{,\phi\phi}\right)^2 + 2\mu\left(-w_{,ss}\right)\left(\frac{\cos\delta}{s^2\sin^2\delta}v_{,\phi} - \frac{1}{s}w_{,s}\right.$$

$$\left. - \frac{1}{s^2\sin^2\delta}w_{,\phi\phi}\right) + 2(1-\mu)\left(\frac{\cos\delta}{s\sin\delta}v_{,s} - \frac{\cos\delta}{s^2\sin\delta}v - \frac{1}{s\sin\delta}w_{,s\phi}\right.$$

$$\left.\left. + \frac{1}{s^2\sin\delta}w_{,\phi}\right)^2\right]s\sin\delta\,ds\,d\phi \qquad (1)$$

where $C = \frac{Eh}{1-\mu^2}$ and $D = \frac{Eh^3}{12(1-\mu^2)}$. The first integral in equation (1) gives the shell extensional energy and the second integral gives the shell bending energy.

The kinetic energy of a conical shell may be written in the following general form:

$$T = \frac{\rho h}{2}\int_0^{2\pi}\int_{s_1}^{s_2}\left(u_{,t}^2 + v_{,t}^2 + w_{,t}^2\right)s\sin\delta\,ds\,d\phi \qquad (2)$$

It is of interest to note that these strain and kinetic energy expressions (eqs. (1) and (2)) reduce (when $\delta = 90^{o}$) to the expressions obtained for the classic flat circular plate with a hole in the middle.

Assumed functions.- Functions of the following form satisfy the model geometric constraints and in addition contain terms that define the zero frequency rigid body modes of the shell (three translations and three rotations):

$$\left.\begin{aligned} u(s,\phi,t) &= \sum_k a_k(t)\left(\frac{s}{s_2}\right)^k \cos n\phi + \sum_k d_k(t)\left(\frac{s}{s_2}\right)^k \sin n\phi \\ v(s,\phi,t) &= \sum_k b_k(t)\left(\frac{s}{s_2}\right)^k \sin n\phi + \sum_k e_k(t)\left(\frac{s}{s_2}\right)^k \cos n\phi \\ w(s,\phi,t) &= \sum_k c_k(t)\left(\frac{s}{s_2}\right)^k \cos n\phi + \sum_k f_k(t)\left(\frac{s}{s_2}\right)^k \sin n\phi \end{aligned}\right\} \tag{3}$$

where $a_k(t)$, $b_k(t)$, $c_k(t)$, $d_k(t)$, $e_k(t)$, and $f_k(t)$ are arbitrary coefficients (amplitude functions); k is a summation index; and n is the circumferential mode number.

Substituting equations (3) into equations (1) and (2) and performing the indicated operations produces two identical, uncoupled sets of energy expressions, one set as functions of a_k, b_k, and c_k, the other set as functions of d_k, e_k, and f_k. Thus, it is possible to omit one series (i.e., the second series) in each of the functions without loss of generality but at a considerable saving in computer space and program complexity. Therefore, the assumed functions used in this investigation are:

$$\left.\begin{aligned} u(s,\phi,t) &= \sum_k a_k(t)\left(\frac{s}{s_2}\right)^k \cos n\phi \\ v(s,\phi,t) &= \sum_k b_k(t)\left(\frac{s}{s_2}\right)^k \sin n\phi \\ w(s,\phi,t) &= \sum_k c_k(t)\left(\frac{s}{s_2}\right)^k \cos n\phi \end{aligned}\right\} \tag{4}$$

where $a_k(t) = \bar{a}_k \cos \omega t$; $b_k(t) = \bar{b}_k \cos \omega t$; $c_k(t) = \bar{c}_k \cos \omega t$. Thus, the modal functions assumed for this investigation to represent the inplane and normal displacements u, v, and w are products of trigonometric functions and power series with arbitrary coefficients.

General form of frequency equation.- The equations of motion are obtained by substituting equations (4) into equations (1) and (2) and using the relations

$$\frac{\partial}{\partial a_j}\left[U\left(a_k,b_k,c_k\right) - \omega^2 T\left(a_k,b_k,c_k\right)\right] = \frac{\partial}{\partial b_j}\left[U\left(a_k,b_k,c_k\right) - \omega^2 T\left(a_k,b_k,c_k\right)\right]$$

$$= \frac{\partial}{\partial c_j}\left[U\left(a_k,b_k,c_k\right) - \omega^2 T\left(a_k,b_k,c_k\right)\right] = 0 \qquad (5)$$

The operations represented by equation (5) produce the familiar eigenvalue-eigenvector formulation which can be written in matrix form as follows:

$$\left[\begin{array}{c|c|c} \alpha & \beta & \gamma \\ \hline \beta' & \theta & \lambda \\ \hline \gamma' & \lambda' & \kappa \end{array}\right]\left\{\begin{array}{c} a_k \\ b_k \\ c_k \end{array}\right\} - \omega^2 \left[\begin{array}{c|c|c} \eta & 0 & 0 \\ \hline 0 & \epsilon & 0 \\ \hline 0 & 0 & \psi \end{array}\right]\left\{\begin{array}{c} a_k \\ b_k \\ c_k \end{array}\right\} = \left\{\begin{array}{c} 0 \\ 0 \\ 0 \end{array}\right\} \qquad (6)$$

where each symbol inside the matrices represents a submatrix whose elements are presented in the appendix. The superscript prime denotes the transpose of a matrix.

METHOD OF SOLUTION OF THE EIGENVALUE PROBLEM

The frequency equation was programed for solution on a large digital computer. The solution technique is of the Jacobi type. (See ch. 3 of ref. 5.) This method of solution yields eigenvalues (frequencies) and associated eigenvectors which can be used directly to obtain theoretical mode shapes for each displacement, normalized to any desired reference.

When using this procedure the investigator must decide on the number of terms to be used in each displacement series in order to insure that the answers obtained are converged in the region of interest (say, for example, the three lowest meridional modes for values of circumferential modes up to 15). The method used in this paper was to increase the number of terms in each series until the change in frequency per term added became

negligible in the region of interest. The results of a typical convergence test are shown in table I. Table I presents the calculated frequencies for several combinations of meridional and circumferential mode numbers, m and n, as the number of terms in each series is increased. An examination of table I indicates that the frequencies obtained with 12 terms in each series vary less than 0.15 percent from those obtained for 15 terms in each series; therefore, the frequencies obtained for 12 terms can be considered converged.

The frequencies presented in table I were obtained by using 28-significant-figure; floating-point arithmetic. Identical frequencies were obtained by using 15 significant figures for up to 10 terms in each displacement series. For applications using more than 10 terms in each series, numerical significance was sometimes lost in the 15-figure calculations. Therefore, it appears that single precision calculations would be sufficient for most applications; however, to insure fully converged results over a wide range of model geometries, 28-figure calculations were used for all values presented herein.

ANALYTICAL RESULTS AND DISCUSSION

In the course of this investigation, frequencies and mode shapes were computed for a variety of shell geometries and materials; an examination of these results indicated that several points of interest existed. Therefore, for the purpose of discussion, one typical shell was selected, its frequencies and mode shapes were determined, and, in addition, pertinent parameters were varied analytically in order to illustrate the various points of interest.

Frequencies and Mode Shapes

The analysis previously described was applied to an 0.0635-cm-thick aluminum-alloy conical shell having a 60° semivertex angle and shell truncation ratio r_1/r_2 of 1/8. The frequency results are presented in figure 2 as solid curves faired through discrete frequency values obtained for various combinations of modal numbers. For all data presented herein the meridional mode number m is defined to be the order of occurrence of resonant frequencies for a given value of circumferential mode number n starting at the lowest value; that is, m = 0, lowest frequency; m = 1, second lowest frequency, and so forth. Abrupt changes in general curvature are seen to occur in each meridional mode curve; that is, n = 4, m = 0; n = 5, m = 1; n $\approx$ 6, m = 2; and so forth.[1] The general character of the curves in these regions indicate the joining of two separate curves, each

[1]In order to define more accurately the curves in these regions, frequencies were obtained for noninteger values of n. Although noninteger values of n do not have a direct physical interpretation, frequency equation (6) is continuous for all finite values of n.

having its own characteristics. Hu, Gormley, and Lindholm in reference 2 have shown that an approximate inextensional analysis yields good frequency agreement with experimentally determined frequencies for small values of n when $m = 0$ or 1. An inextensional analysis similar to that of reference 2 (mode shape assumptions of the form used in the present investigation were used) was applied to this conical shell with the results shown as dashed curves faired through discrete frequency values in figure 2. In figure 2 the inextensional analysis and the present analysis are seen to coincide for small n when $m = 0$ and 1 and that the curvature change for $m > 1$ occurs in the region where the inextensional analysis intersects the present analysis curves. It is of interest to note that the phenomenon associated with the intersection of the inextensional analysis and the $m > 1$ curves occurred for each of the model geometries used in this investigation and that the degree of change in appearance of the curves was highly dependent on the model geometry. Also, the stiffness matrix tangential v modal series elements (θ in the appendix for values of $k = 0$ and 1) are identically the stiffness parameters of the inextensional analysis (ref. 2).

Another aspect of conical shell behavior was obtained by examining the calculated meridional w mode shapes. Calculated mode shapes for several combinations of mode numbers in the regions of interest (small n) are shown in figure 3. As can be seen in this figure, the mode shape (for a given value of m) changes character as n increases. In addition, the change in meridional curvature increases sharply as m increases. For n greater than 6, the meridional curvature increases gradually with increasing n while retaining the characteristic shape shown for $n = 6$ in figure 3.

Thus, a conical shell is seen to exhibit two distinct vibration characteristics and the transformation from one to the other is accompanied by both abrupt curvature changes in the frequency—mode-number curves (fig. 2) and a marked change in the characteristic shape of the meridional mode (fig. 3). For convenience of discussion and to conform with previous definitions (refs. 2 and 6, for example) these two regions of response will be called inextensional and regular for small n and large n, respectively. These two regions are defined as follows:

Inextensional – (a) $m = 0$, $m = 1$ – that portion of the curve for frequency plotted against circumferential mode number which can be approximated by an inextensional analysis, (b) $m > 1$ – that portion of the meridional mode curve to the left (small n) of the intersection of the meridional mode curve and the second mode inextensional analysis curve

Regular – all values of m – that portion of the curve to the right (large n) of the region designated inextensional

Effect of Shell Truncation Ratio

In developing this analysis a characteristic term of the form $1 - (r_1/r_2)^{j+k}$ appeared in essentially all the matrix elements; thus, a model geometry influence is indicated on the shape of the curves for frequency plotted against modal number. This term contains the shell truncation ratio r_1/r_2. The effect of the truncation ratio was evaluated by varying r_1 while holding all other values constant. The results are shown in figure 4. These results show that the shell truncation ratio has a pronounced effect on the shape of the frequency curves particularly for values of $m = 1$ and 2. The primary influence of the ratio appears to be in determining the range of n numbers for which the shell response falls in the inextensional region – that is, the smaller the ratio r_1/r_2 the quicker the shell passes from the inextensional to the regular mode of vibrations.

COMPARISONS WITH EXPERIMENT

Experimental Data

Data sources.- The literature contains several sets of experimentally determined frequencies for conical shells with free edges. In this paper, three of these sets of data (refs. 1, 6, and 7) are combined with previously unpublished experimental data obtained at the Langley Research Center to provide a reasonably wide variety of model geometries, materials, and so forth, with which to evaluate the present analysis. Table II presents a summary of the sources of experimental data and the model dimensions and material properties used in the analysis. The experimental data are represented with symbols in figures 5 to 8 for sources (1) to (4) (table II), respectively. Also, the unpublished data, sources (1) and (3), are presented in tables III and IV, respectively.

Boundary restraint simulation and model excitation.- Achieving a truly free-free boundary condition in laboratory experiments is virtually impossible; therefore, it is necessary to use a mounting system that has minimum restraint. For conical shells for which there is such a large range of vibratory behavior it would appear that a combination of boundary restraint methods may be necessary. In addition to boundary restraint effects on the vibration characteristics the manner in which the model is excited can influence the results obtained, see for example the discussion in reference 6.

Data source (1): The model for data source (1) was tested with the small radius down and (1) resting on a pad of soft hair or (2) suspended by eight evenly spaced soft rubber bands at the major radius. In both cases excitation was with an air shaker (no attachment between model and shaker). As shown in table III, the hair pad support produced consistently lower frequencies for small values of n and $m = 0$ than were obtained for the rubber band suspension, whereas the $m = 1$ frequencies could not be clearly excited when the hair pad support was used.

Data source (2): The models for data source (2) were tested with the large radius up and suspended by soft rubber bands having various combinations of stiffness and spacing. (See ref. 6 for details.) Model excitation was with an air shaker.

Data source (3): The models for data source (3) were tested with the large radius down and supported with cords passed around the model along the slant length. This manner of model support eliminated one mode of vibration, that is, $n = 2$, $m = 1$. (See table IV and the discussion in ref. 7.) The models were excited with an electric shaker and with an air shaker. The very large differences in frequency obtained by the two excitation methods are evident in table IV.

Data source (4): The models for data source (4) were tested with the large radius up and resting on three equally spaced soft rubber pads at the small radius. Excitation was by magnetic induction. Although it is stated in reference 1 that the boundary restraint did not influence the data, it is of interest to point out that the lowest frequency obtained for the $m = 1$ curve was for $n = 6$, except for the model having the smallest semivertex angle, which indicates a restraint influence similar to that noted for test data in sources (1) and (3).

Frequency Comparisons

The analysis of this paper was applied to each shell and the frequency results are presented in figures 5 to 8 as solid lines. Frequency agreement between experiment and analysis is considered to be excellent for all comparisons except where boundary restraints and/or excitation techniques influence the experimental data (small values of n and $m = 0$ and 1). The agreement in this region is improved when adequate precautions are taken in the experimental test procedures. One other region of less than good agreement between theory and experiment occurs for large values of n and $m = 1$ and 2 in figure 9(c). There is no apparent explanation for this discrepancy; however, it should be noted that the experimentally obtained trend for data to approach the $m = 0$ data for $n > 16$ occurs only for this particular model.

Mode Shape Comparisons

Experimentally measured meridional normal w mode shapes were determined for two models, the aluminum-alloy 60° cone and the cold rolled steel 45.1° cone (ref. 1). For both models, noncontacting displacement-sensing transducers were used to sense the vibration motion; for the cone in reference 1, the probes were fixed and for the aluminum-alloy cone the probe was servocontrolled as described in reference 8. The mode shape data are presented in figures 9 and 10. In these figures normalized analytical meridional mode shapes are shown as solid curves and normalized experimental mode shapes as dashed lines. In general, all comparisons show good agreement, with the model curvature

and theoretical curvature being similar although in some comparisons the predicted and measured displacements are different. Part of the difference in deflections is probably due to such things as signal error, boundary restraints, and local imperfections in the model, particularly near the ends where large vibratory motion generally occurs.

CONCLUSIONS

An analytical procedure for predicting the vibratory behavior, both frequencies and mode shape, of free-free truncated conical shells has been described. The procedure utilizes the Rayleigh-Ritz procedure by using simple power series to approximate the meridional mode shapes and trigonometric functions to approximate the circumferential mode shapes. The results of this analysis and comparisons with experimentally determined frequencies and mode shapes lead to the following conclusions:

1. Conical shells have two distinct modes of vibration; as defined herein, they are inextensional (small n (circumferential mode number)) and regular (large n). The demarcation between the two modes is quite clear in frequency-modal-number plots.

2. In the inextensional region, the meridional curvature increases rapidly with increasing m (meridional mode number) and n, whereas in the regular region the meridional curvature increases gradually with increasing n.

3. The shell truncation ratio (minimum radius/maximum radius) was found to influence the range of n required for the shell to pass from the inextensional to the regular vibration mode. The rate decreases as the shell truncation ratio decreases.

4. Frequency agreement between the results of the present analysis and the results from experimental studies was found to be excellent for models having the following ranges of parameters: (1) semivertex angles from 3.2° to 60.5°, (2) shell truncation ratio r_1/r_2 from 1/8 to 6/7, (3) shell thicknesses from 0.0178 cm to 0.0813 cm, (4) major radius r_2 from 15.43 cm to 60.96 cm, and (5) materials – aluminum alloy, cold rolled steel, and stainless steel.

5. Meridional mode shape agreement between theoretical and experimental values was found to be very good for two different models.

Langley Research Center,
National Aeronautics and Space Administration,
Langley Station, Hampton, Va., May 16, 1968,
124-08-05-02-23.

APPENDIX

MATRIX ELEMENTS FOR RAYLEIGH-RITZ VIBRATION ANALYSIS

This appendix contains the frequency equation corresponding to equation (6) and detailed expressions for the matrix elements of this equation. The frequencies may be obtained from this equation by setting the determinant of the amplitude functions a_k, b_k, and c_k equal to zero. In matrix form this yields:

$$\left\| \left[\begin{array}{c|c|c} \alpha & \beta & \gamma \\ \hline \beta' & \theta & \lambda \\ \hline \gamma' & \lambda' & \kappa \end{array}\right] - \omega^2 \left[\begin{array}{c|c|c} \eta & 0 & 0 \\ \hline 0 & \epsilon & 0 \\ \hline 0 & 0 & \psi \end{array}\right] \right\| = 0 \tag{A1}$$

where the prime denotes transpose and α, β, . . . ψ each represent a submatrix whose elements are specified as follows:

$$\alpha_{jk} = \left[\left[jkC_{11} + C_{22} + (j + k)C_{12} + \frac{n^2}{\sin^2 \delta} C_{66}\right] \frac{1}{j + k} \left[1 - \left(\frac{r_1}{r_2}\right)^{j+k}\right]\right]$$

$$\beta_{jk} = \frac{n}{\sin \delta}\left[\left[C_{22} + jC_{12} - (k - 1)C_{66}\right] \frac{1}{j + k} \left[1 - \left(\frac{r_1}{r_2}\right)^{j+k}\right]\right]$$

$$\gamma_{jk} = \frac{\cos \delta}{\sin \delta}\left[\left(C_{22} + jC_{12}\right) \frac{1}{j + k} \left[1 - \left(\frac{r_1}{r_2}\right)^{j+k}\right]\right]$$

$$\theta_{jk} = \left[\left[\frac{n^2}{\sin^2 \delta} C_{22} + (j - 1)(k - 1)C_{66}\right] \frac{1}{j + k} \left[1 - \left(\frac{r_1}{r_2}\right)^{j+k}\right] + \frac{\cos^2 \delta}{\sin^2 \delta}\left[\frac{n^2}{\sin^2 \delta} D_{22}\right.\right.$$

$$\left.\left. + (j - 1)(k - 1)D_{66}\right] \frac{\sin^2 \delta}{r_2^2(j + k - 2)} \left[1 - \left(\frac{r_1}{r_2}\right)^{j+k-2}\right]\right]$$

APPENDIX

$$\lambda_{jk} = \frac{n \cos \delta}{\sin^2 \delta}\left[C_{22}\frac{1}{j+k}\left[1 - \left(\frac{r_1}{r_2}\right)^{j+k}\right] + \left[\left(\frac{n^2}{\sin^2 \delta} - k\right)D_{22} - k(k-1)D_{12} + (k-1)(j-1)D_{66}\right]\frac{\sin^2 \delta}{(j+k-2)r_2^2}\left[1 - \left(\frac{r_1}{r_2}\right)^{j+k-2}\right]\right]$$

$$\kappa_{jk} = \left[\frac{\cos^2 \delta}{\sin^2 \delta}C_{22}\frac{1}{j+k}\left[1 - \left(\frac{r_1}{r_2}\right)^{j+k}\right] + \left[jk(j-1)(k-1)D_{11} + \left(\frac{n^2}{\sin^2 \delta} - j\right)\left(\frac{n^2}{\sin^2 \delta} - k\right)D_{22} - \left[j(j-1)\left(\frac{n^2}{\sin^2 \delta} - k\right) + k(k-1)\left(\frac{n^2}{\sin^2 \delta} - j\right)\right]D_{12} + \frac{n^2}{\sin^2 \delta}(j-1)(k-1)D_{66}\right]\left(\frac{\sin^2 \delta}{(j+k-2)r_2^2}\right)\left[1 - \left(\frac{r_1}{r_2}\right)^{j+k-2}\right]\right]$$

$$\eta = \epsilon = \psi = \left[\frac{\rho h r_2^2}{\sin^2 \delta (j+k+2)}\left[1 - \left(\frac{r_1}{r_2}\right)^{j+k+2}\right]\right]$$

where

$$C_{11} = C_{22} = \frac{Eh}{1-\mu^2} \qquad D_{11} = D_{22} = \frac{Eh^3}{12(1-\mu^2)}$$

$$C_{12} = \mu C_{11} \qquad D_{12} = \mu D_{11}$$

$$C_{66} = \frac{1-\mu}{2}C_{11} \qquad D_{66} = 2(1-\mu)D_{11}$$

and

$$\frac{1}{j+k}\left[1 - \left(\frac{r_1}{r_2}\right)^{j+k}\right] = \ln \frac{r_2}{r_1} \qquad (j+k=0)$$

APPENDIX

$$\frac{\sin^2 \delta}{(j + k - 2)r_2^2}\left[1 - \left(\frac{r_1}{r_2}\right)^{j+k-2}\right] = \frac{\sin^2 \delta}{r_2^2} \ln \frac{r_2}{r_1} \qquad (j + k = 2)$$

A machine computer program, written in FORTRAN IV language, was developed for use on the Control Data 6600 computer system or its equivalent to solve the frequency equations.

REFERENCES

1. Hu, W. C. L.; Gormley, J. F.; and Lindholm, U. S.: Flexural Vibrations of Conical Shells With Free Edges. NASA CR-384, 1966.

2. Hu, William C. L.; Gormley, John F.; and Lindholm, Ulric S.: An Experimental Study and Inextensional Analysis of Vibrations of Free-Free Conical Shells. Int. J. Mech. Sci., vol. 9, Mar. 1967, pp. 123-135.

3. Krause, Frederick A.: Natural Frequencies and Mode Shapes of the Truncated Conical Shell With Free Edges. SSD-TR-66-201, U.S. Air Force, Oct. 1966. (Available from DDC as AD 803 426.)

4. Novozhilov, V. V. (P. G. Lowe, transl.): Thin Shell Theory. Second ed., P. Noordhoff Ltd. (Groningen, Neth.), c.1964.

5. Bodewig, E.: Matrix Calculus. Second rev. ed., Interscience Publ., Inc., 1959.

6. Mixson, John S.: Experimental Modes of Vibration of 14^{o} Conical-Frustum Shells With Free Ends. NASA TN D-4428, 1968.

7. Watkins, Jerry D.; and Clary, Robert R.: Vibrational Characteristics of Some Thin-Walled Cylindrical and Conical Frustum Shells. NASA TN D-2729, 1965.

8. Naumann, Eugene C.; and Flagge, Bruce: A Noncontacting Displacement Measuring Technique and Its Application to Current Vibration Testing. Preprint No. 16.18-5-66, Instrum. Soc. Amer., Oct. 1966.

TABLE I.- SERIES CONVERGENCE DETERMINATION

Number of terms in each series	Frequency, hertz, for –														
	m = 0 and n =					m = 1 and n =					m = 2 and n =				
	2	3	4	14	15	2	3	4	14	15	2	3	4	14	15
3	2.702	6.98	12.82	111.5	127.6	31.37	72.6	122	387	443	1010	728	527	2300	2645
5	2.700	6.98	12.73	103.9	117.4	31.46	72.2	117	225	241	718	599	449	417.7	446.5
8	2.699	6.97	12.71	102.5	115.8	31.45	72.16	116.7	202	218	692	598.2	448	334.8	347.6
10	2.698	6.96	12.70	102.2	115.4	31.45	72.14	116.6	201.7	216.8	687	598.1	447.9	326.4	339.2
12	2.697	6.96	12.70	102.1	115.3	31.43	72.08	116.5	201.6	216.8	686.5	598.1	447.8	326.0	339.0
15	2.697	6.96	12.70	102.1	115.3	31.37	71.94	116.4	201.6	216.8	686.0	598.1	447.7	326.0	339.0
Inextensional	2.702	6.99	12.86			31.50	73.2	128.0							

TABLE II.- MODEL DIMENSIONS AND MATERIAL PROPERTIES

Data source	δ, deg	r_1, cm	r_2, cm	r_1/r_2	h, cm	Material	E, GN/m^2	ρ, kg/m^2	μ
(1)									
Langley unpublished (table III)	60	7.62	60.96	1/8	0.0635	Aluminum alloy (6061-T6)	68.95	7.02	0.315
(2)									
Reference 6	14	20.32	35.56	4/7	0.0813	Stainless steel	193.05	20.79	0.3
(NASA TN D-4428)	14	20.32	35.56	4/7	.0432		193.05	20.79	.3
	14	20.32	35.56	4/7	.0221		193.05	20.79	.3
(3)									
Reference 7	3.2	30.48	35.56	6/7	0.0178	Stainless steel	193.05	20.79	0.3
(NASA TN D-2729)	7.4	35.4	35.56	5/7	.0178		193.05	20.79	.3
Langley unpublished	14	20.32	35.56	4/7	.0178		193.05	20.79	.3
(table IV)	24	15.24	35.56	3/7	.0178		193.05	20.79	.3
(4)									
Reference 1	14.2	6.91	15.43	1/2.23	0.0254	Cold rolled steel	203.40	20.29	0.3
(NASA CR-384)	30.2	8.89	20.19	1/2.27	.0254		203.40	20.29	.3
	45.1	10.14	22.76	1/2.25	.0254		203.40	20.29	.3
	60.5	11.28	25.40	1/2.25	.0254		203.40	20.29	.3

TABLE III.- EXPERIMENTAL FREQUENCIES FOR 60° CONICAL SHELL

[Data source (1)]

Circumferential mode number, n	Frequency, hertz, for –		
	m = 0		m = 1
	Suspended at r_2	Supported at r_1	Suspended at r_2
2	4.4	3.4	31.4
3	7.7	7.2	70.7
4	13.6	12.9	118
5	20.1	19.7	
6	27.2	27.1	
7	34.3	34.2	
8	41.9	41.7	
9	50.0	50.0	
10	58.9	58.9	
11	68.4	68.4	
12	78.9	78.9	
13	90.1		
14	102.1		
15	115.4		

TABLE IV.- EXPERIMENTAL FREQUENCIES FOR CONICAL SHELLS

[Data source (3)]

Electric shaker (NASA TN D-2729)			Air shaker (unpublished)	
			Frequency, hertz, for –	
$n_{r1} - n_{r2}$ (a)	Frequency, hertz	n	m = 0	m = 1
	(a) 3.2° cone; $r_1/r_2 = 6/7$			
- - 3	4.3	2	1.1	----
- - 4	7.3	3	2.8	3.6
4 - 5	10.4	4	5.1	7.2
- - 6	14.8	5	8.3	10.3
6 - 7	18.2	6	12.2	14.9
7 - 8	24.6	7	16.8	20.4
8 - 9	30.8	8	22.1	26.2
9 - 10	36.2	9	28.1	33.7
		10	34.5	41.5
	(b) 7.4° cone; $r_1/r_2 = 5/7$			
- - 3	4.8	2	1.1	----
- - 4	8.0	3	3.1	4.6
4 - 5	12.1	4	5.4	7.9
5 - 6	17.0	5	8.9	13.5
5 - 7	22.2	6	12.9	19.2
6 - 8	27.1	7	17.9	26.7
7 - 9	33.8	8	23.4	35.2
7 - 10	39.6	9	29.8	44.7
		10	36.5	54.8
	(c) 14° cone; $r_1/r_2 = 4/7$			
- - 3	5.6	2	1.5	----
3 - 4	9.4	3	3.7	----
4 - 5	12.9	4	6.2	13.2
4 - 6	17.9	5	9.6	18.6
5 - 7	22.0	6	14.1	26.8
5 - 8	28.5	7	20.2	38.1
6 - 9	34.6	8	25.1	----
6 - 10	41.9	9	32.6	----
		10	40.1	----
	(d) 24° cone; $r_1/r_2 = 3/7$			
- - 3	5.8	2	1.6	----
3 - 4	9.4	3	3.9	10.2
3 - 5	13.9	4	6.6	18.9
3 - 6	19.0	5	11.0	29.2
4 - 7	25.1	6	15.5	42.0
5 - 8	31.4	7	21.4	57.6
5 - 9	37.8	8	28.1	74.5
5 - 10	44.8	9	35.5	----
		10	43.4	----

[a] $n_{r1} - n_{r2}$ = Circumferential mode number at small end - Circumferential mode number at large end.

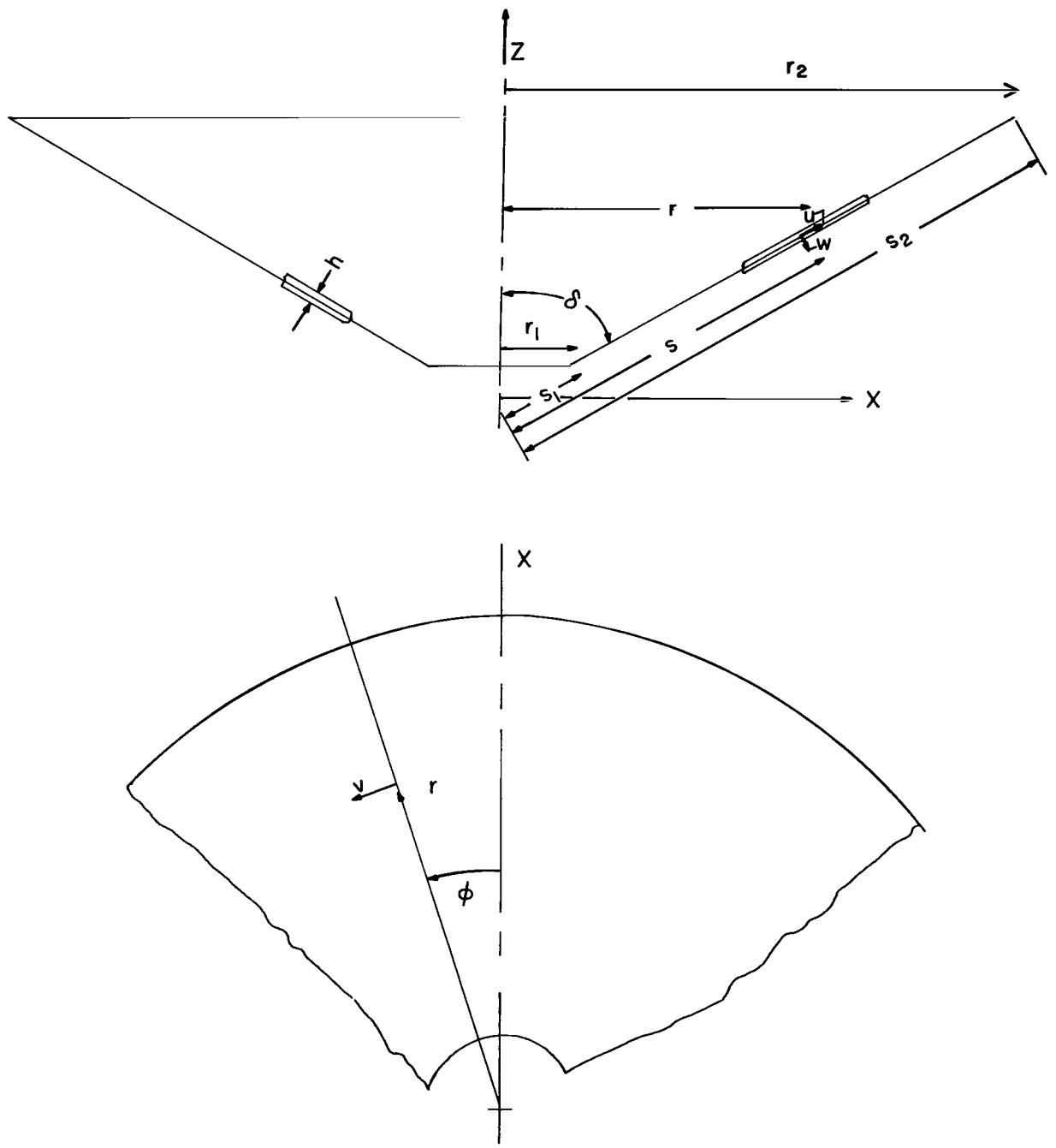

Figure 1.- Coordinate system and modal displacement directions.

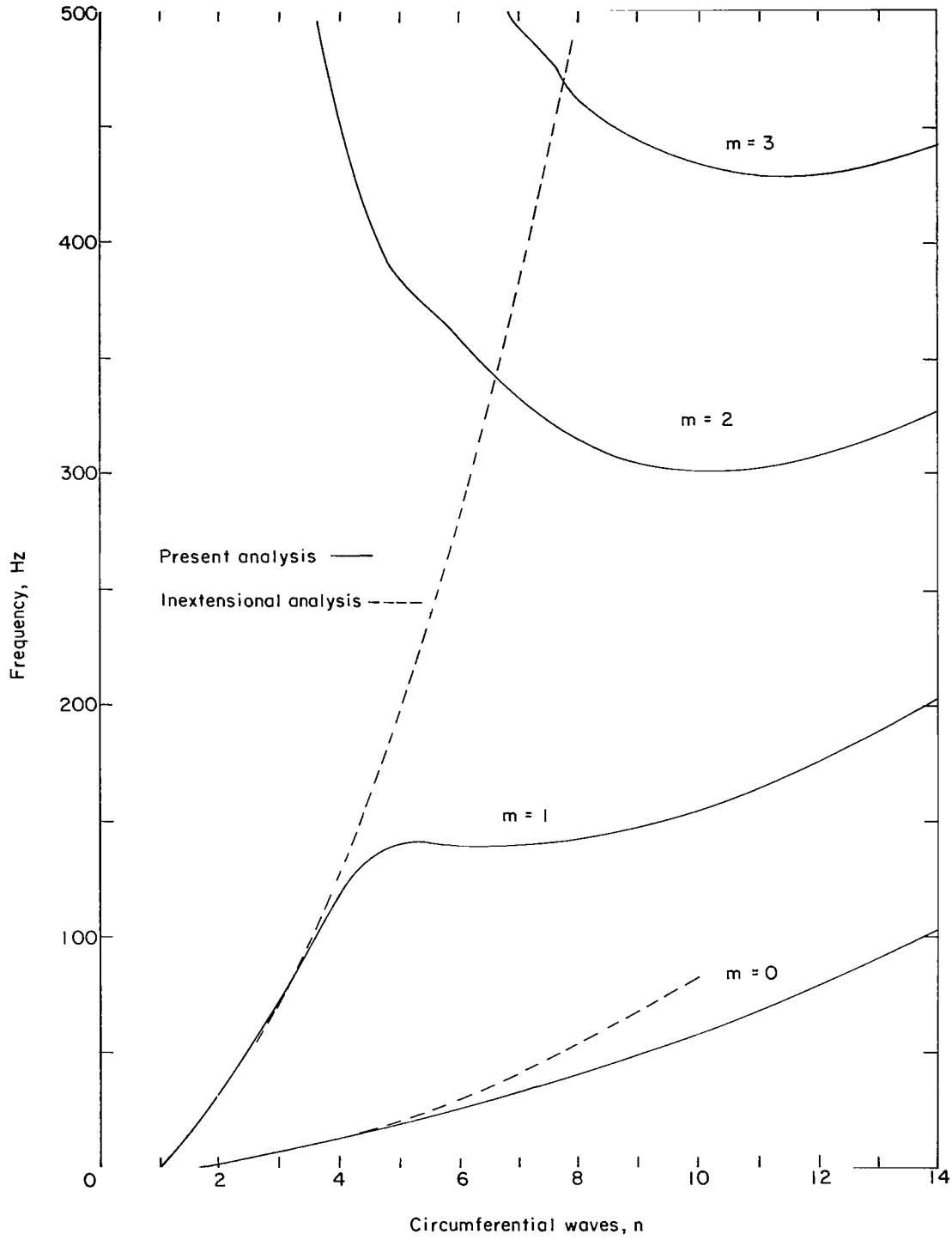

Figure 2.- Results of present analysis and inextensional analysis. $\frac{r_1}{r_2} = \frac{1}{8}$; $\delta = 60^0$.

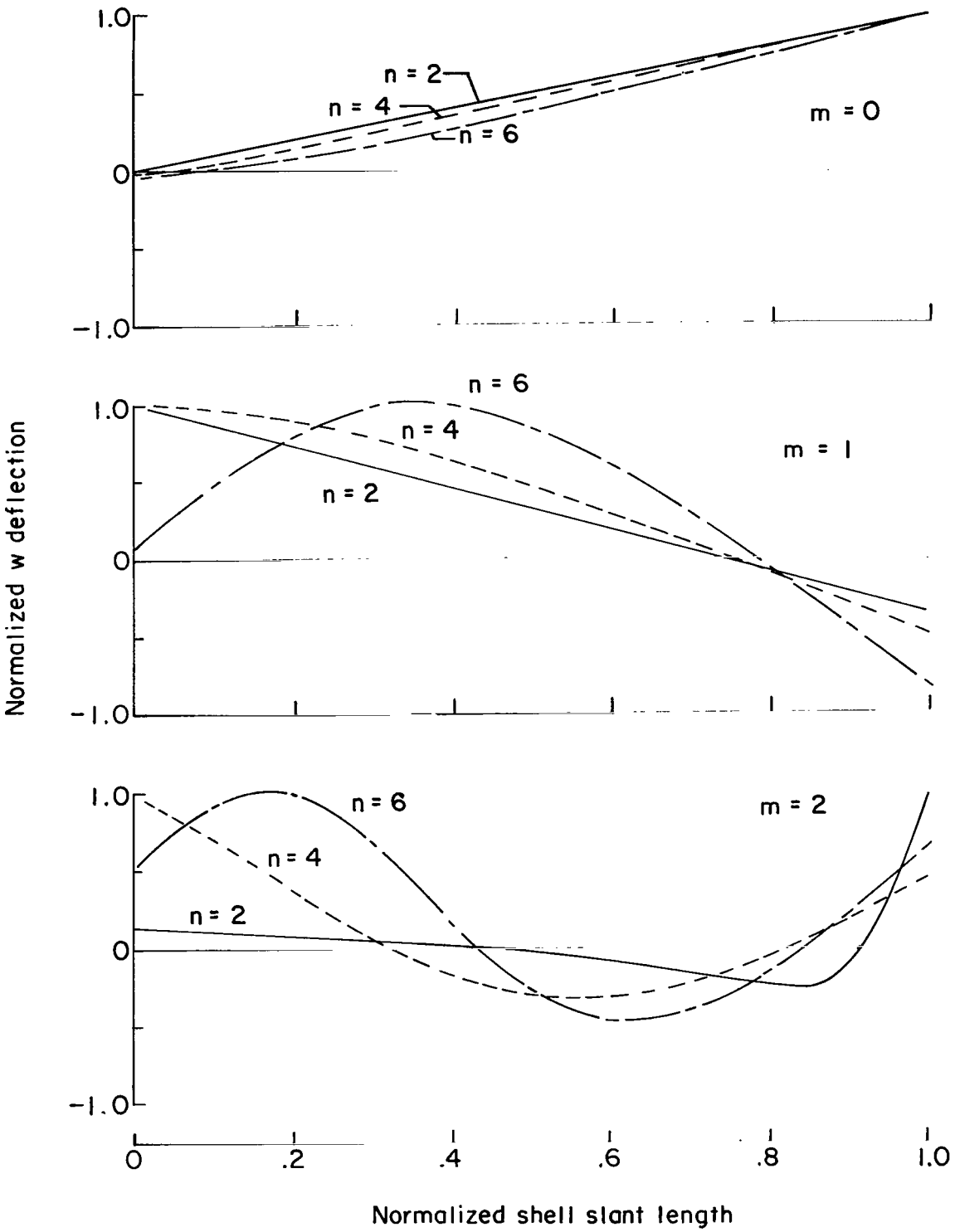

Figure 3.- Variation in w mode shape with increasing circumferential and meridional mode numbers.

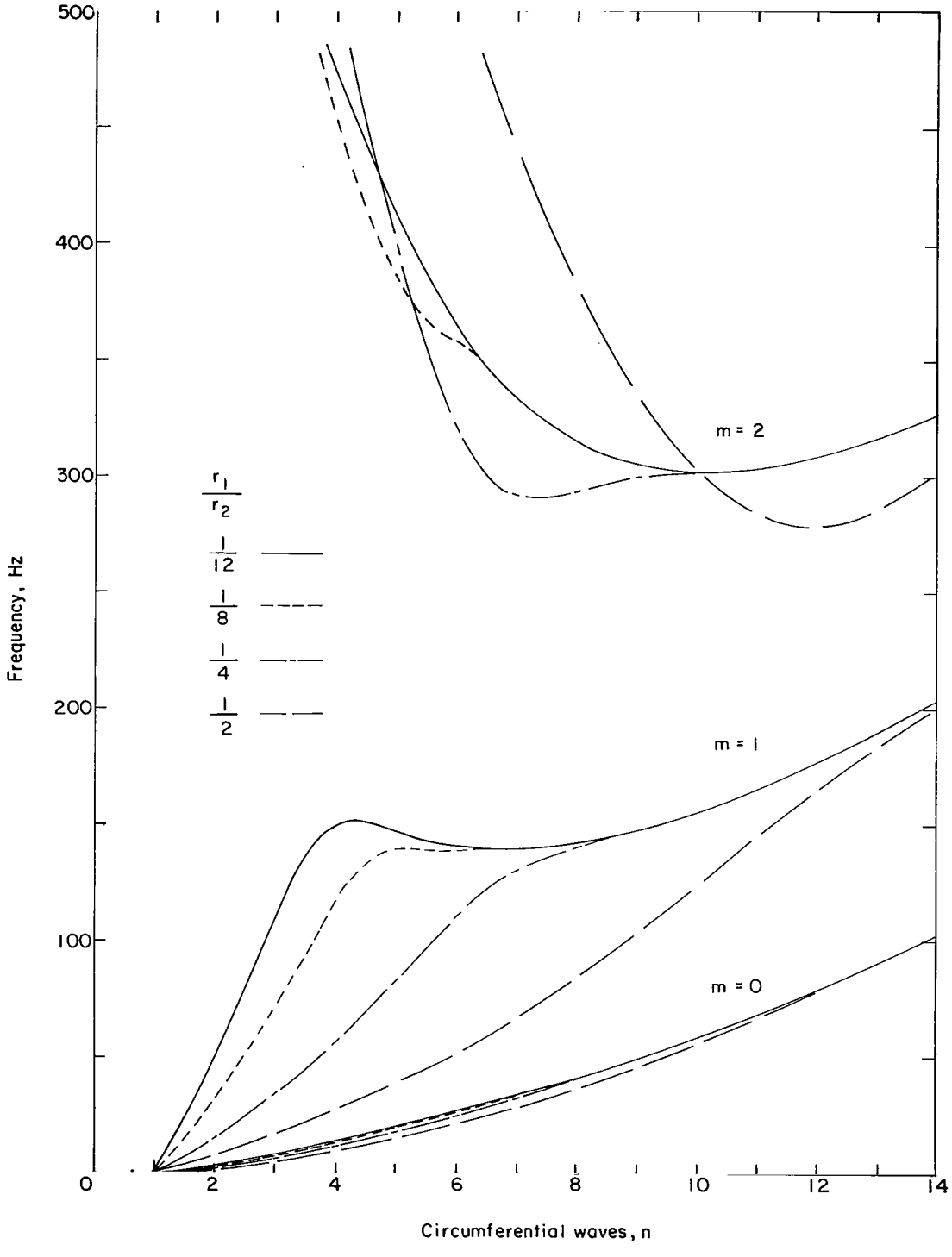

Figure 4.- Effect of truncation ratio $\frac{r_1}{r_2}$. $\delta = 60^0$.

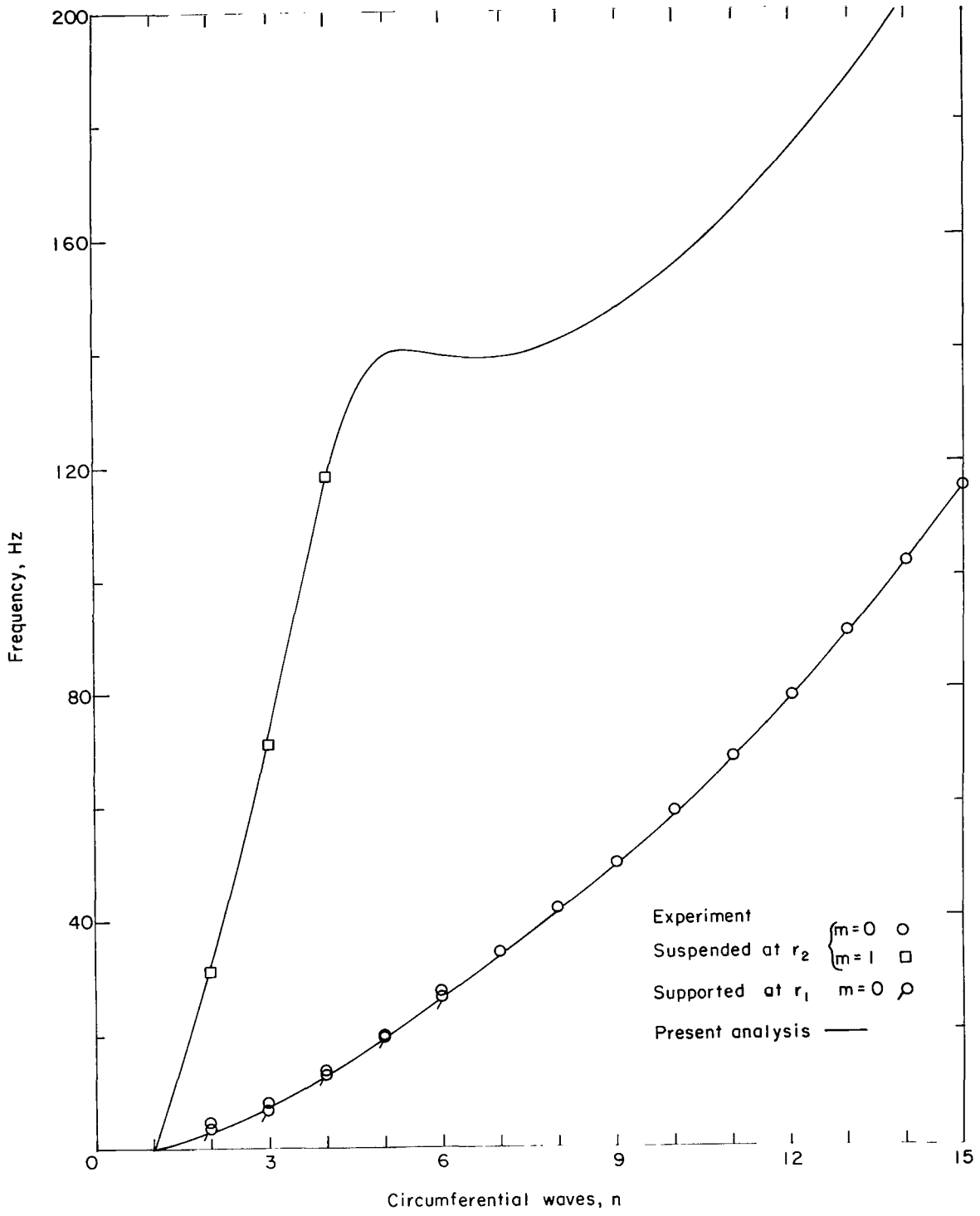

Figure 5.- Comparison of analysis and experiment (data source (1)). $\delta = 60^0$; $\frac{r_1}{r_2} = \frac{1}{8}$; aluminum alloy.

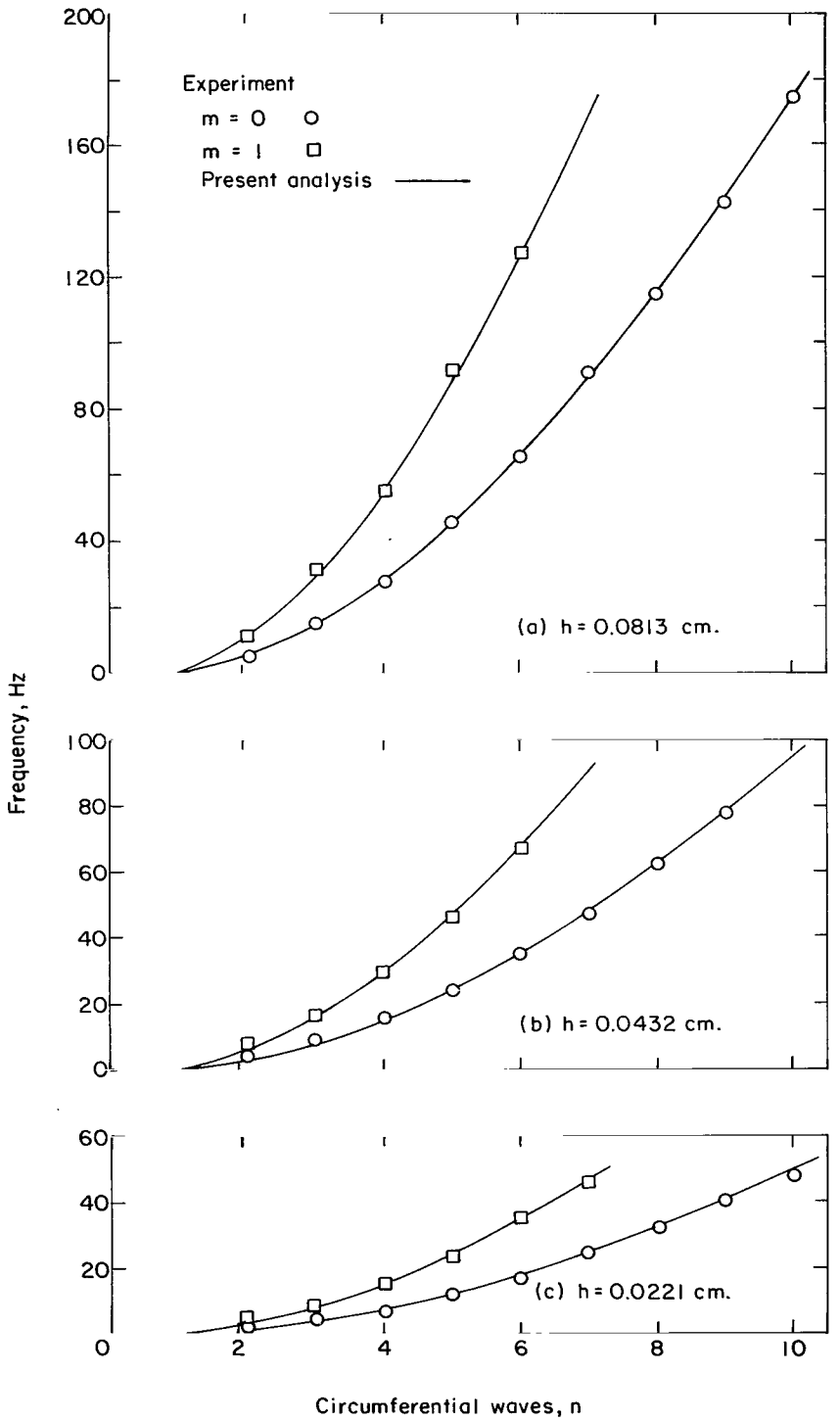

Figure 6.- Comparison of analysis and experiment (data source (2)). $\delta = 14^0$; $\frac{r_1}{r_2} = \frac{4}{7}$.

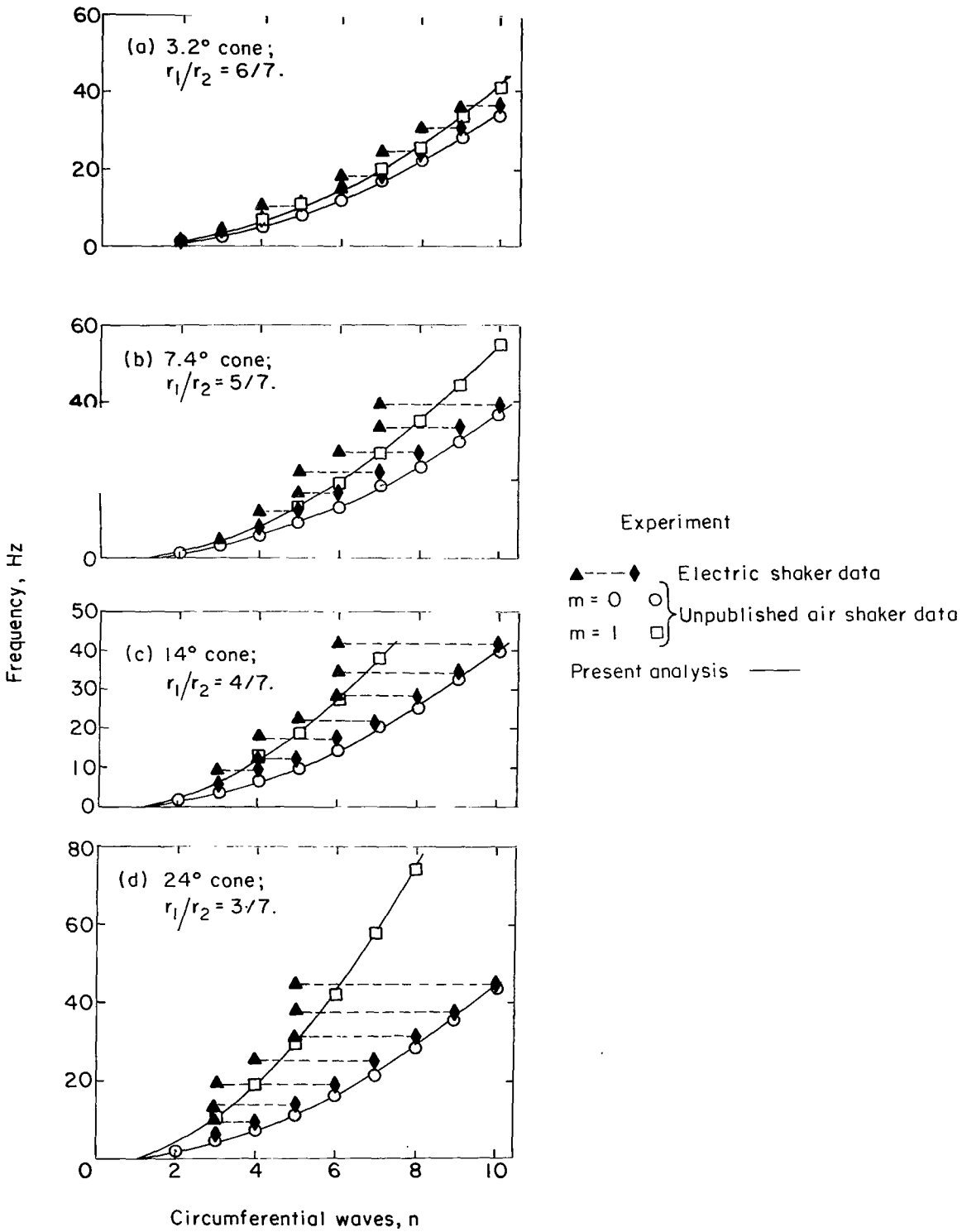

Figure 7.- Comparison of analysis and experiment (data source (3)).

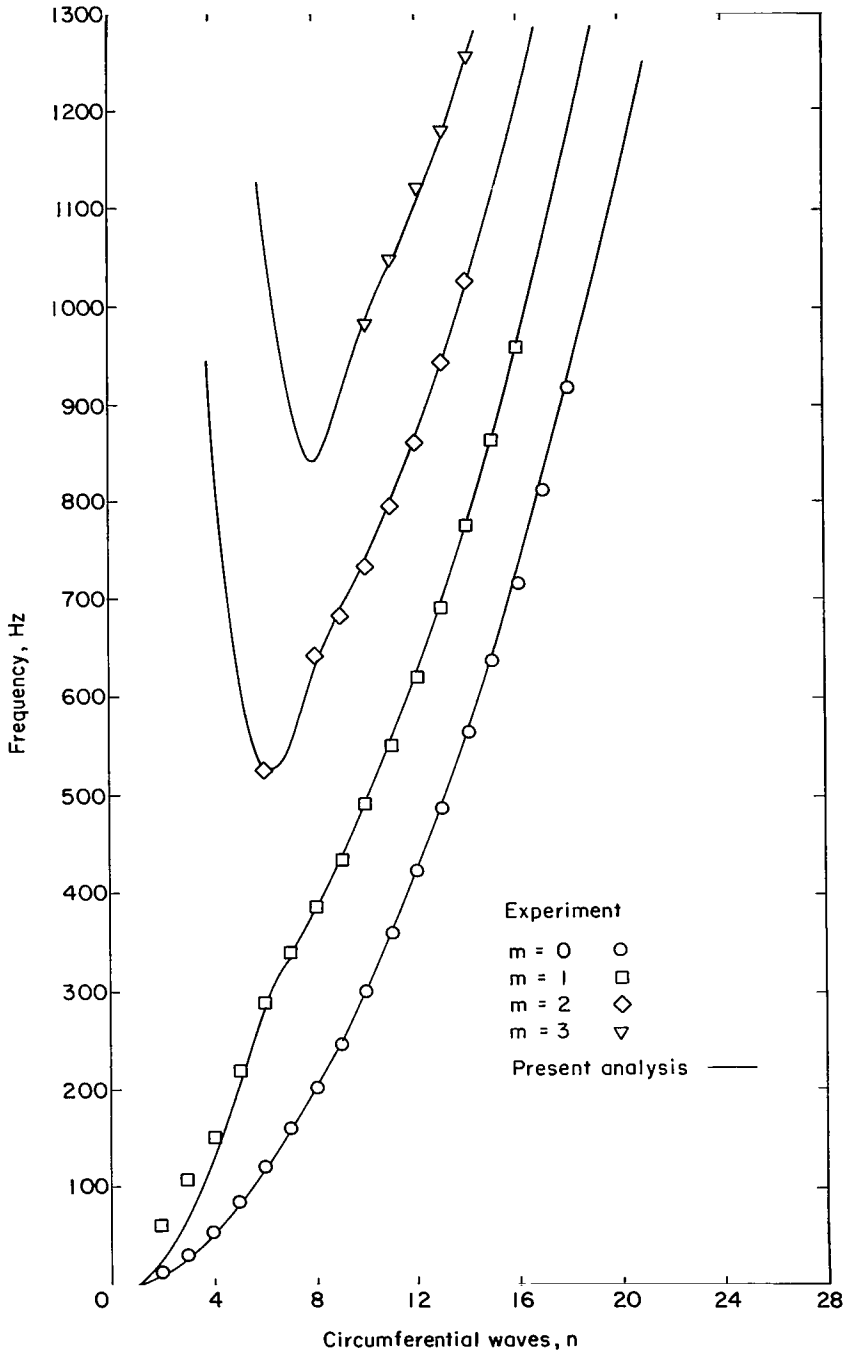

(a) 14.2^0 cone; $\frac{r_1}{r_2} = \frac{1}{2.23}$.

Figure 8.- Comparison of analysis and experiment (data source (4)).

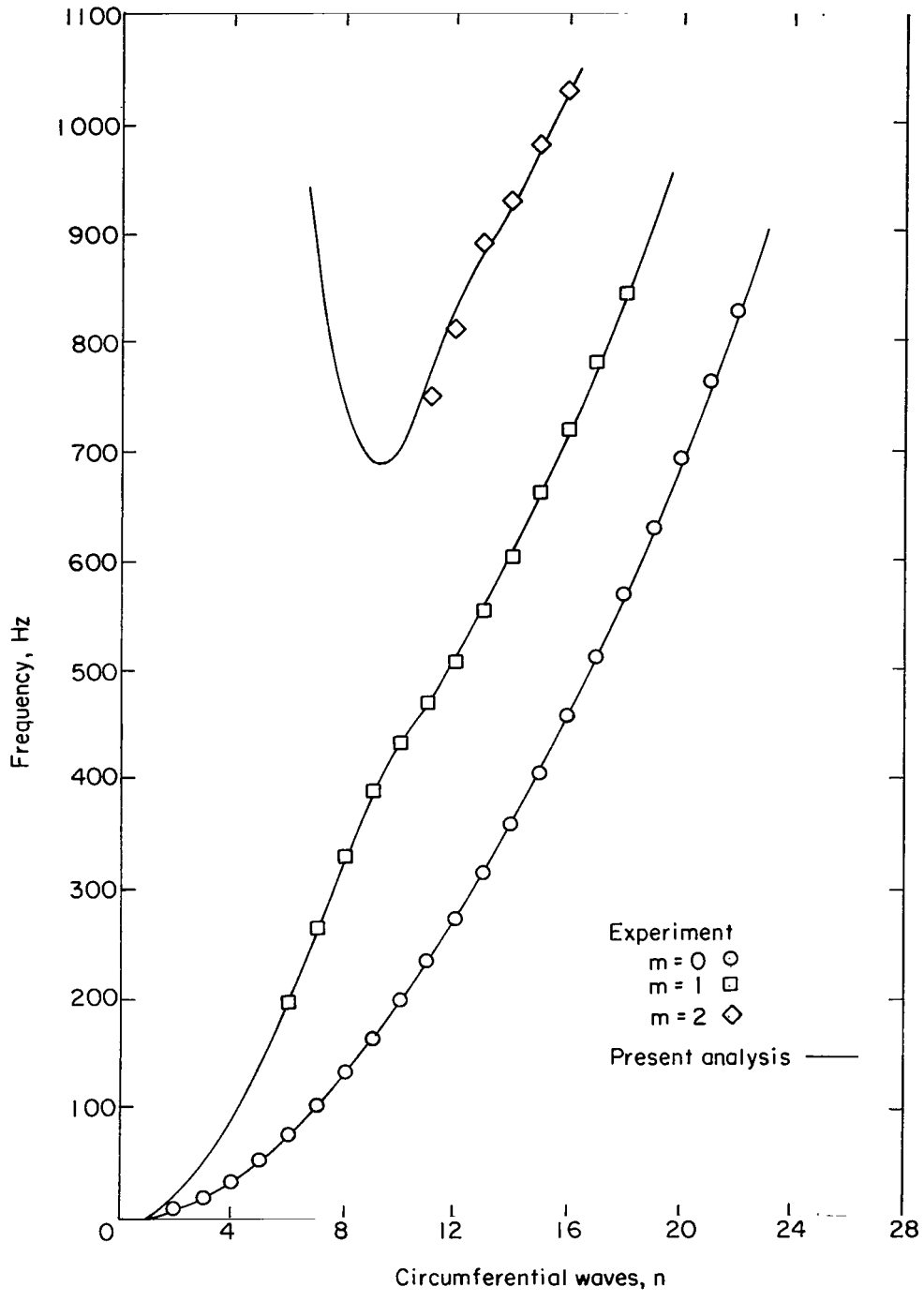

(b) 30.2 cone; $\frac{r_1}{r_2} = \frac{1}{2.27}$.

Figure 8.- Continued.

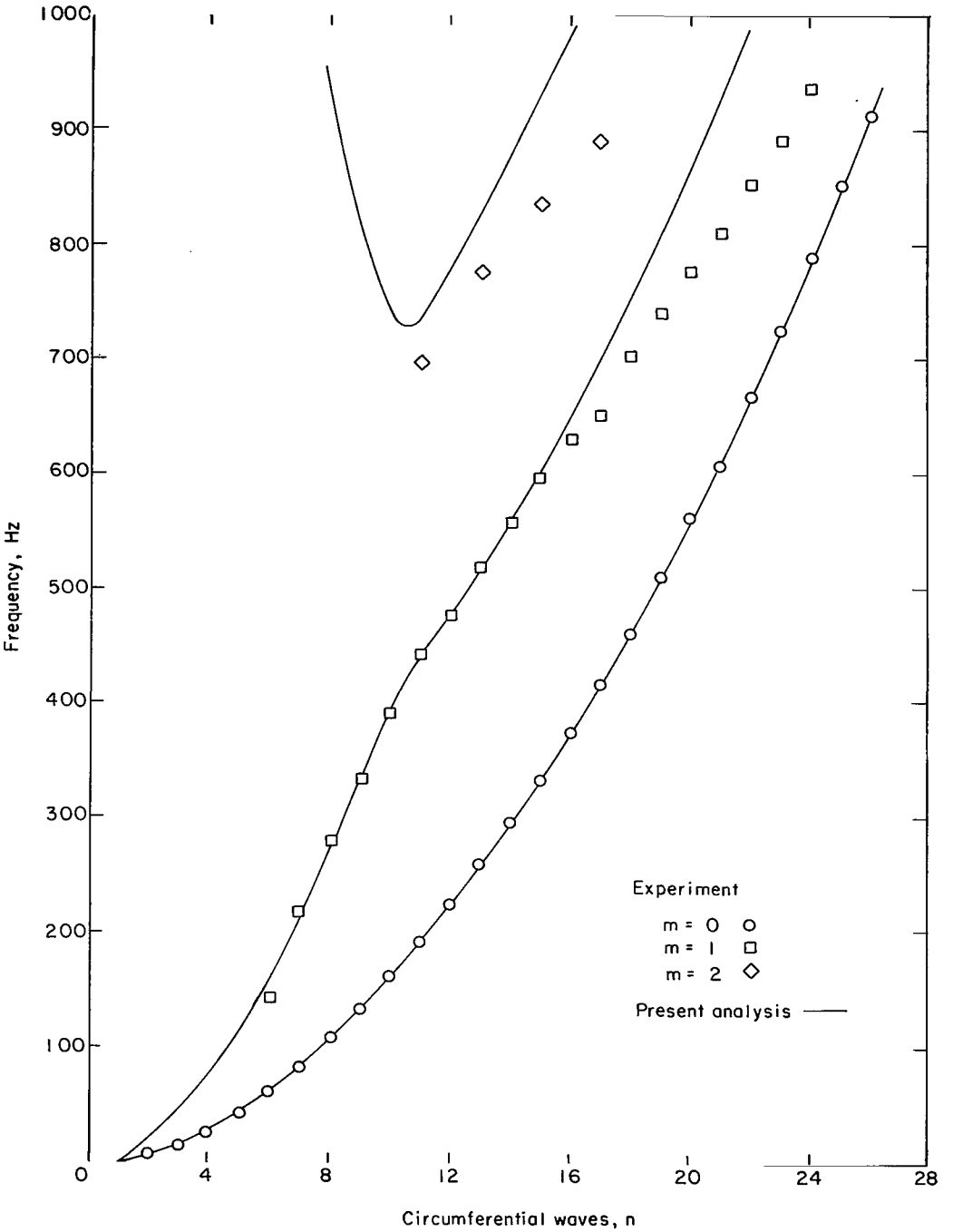

(c) 45.1^0 cone; $\frac{r_1}{r_2} = \frac{1}{2.25}$.

Figure 8.- Continued.

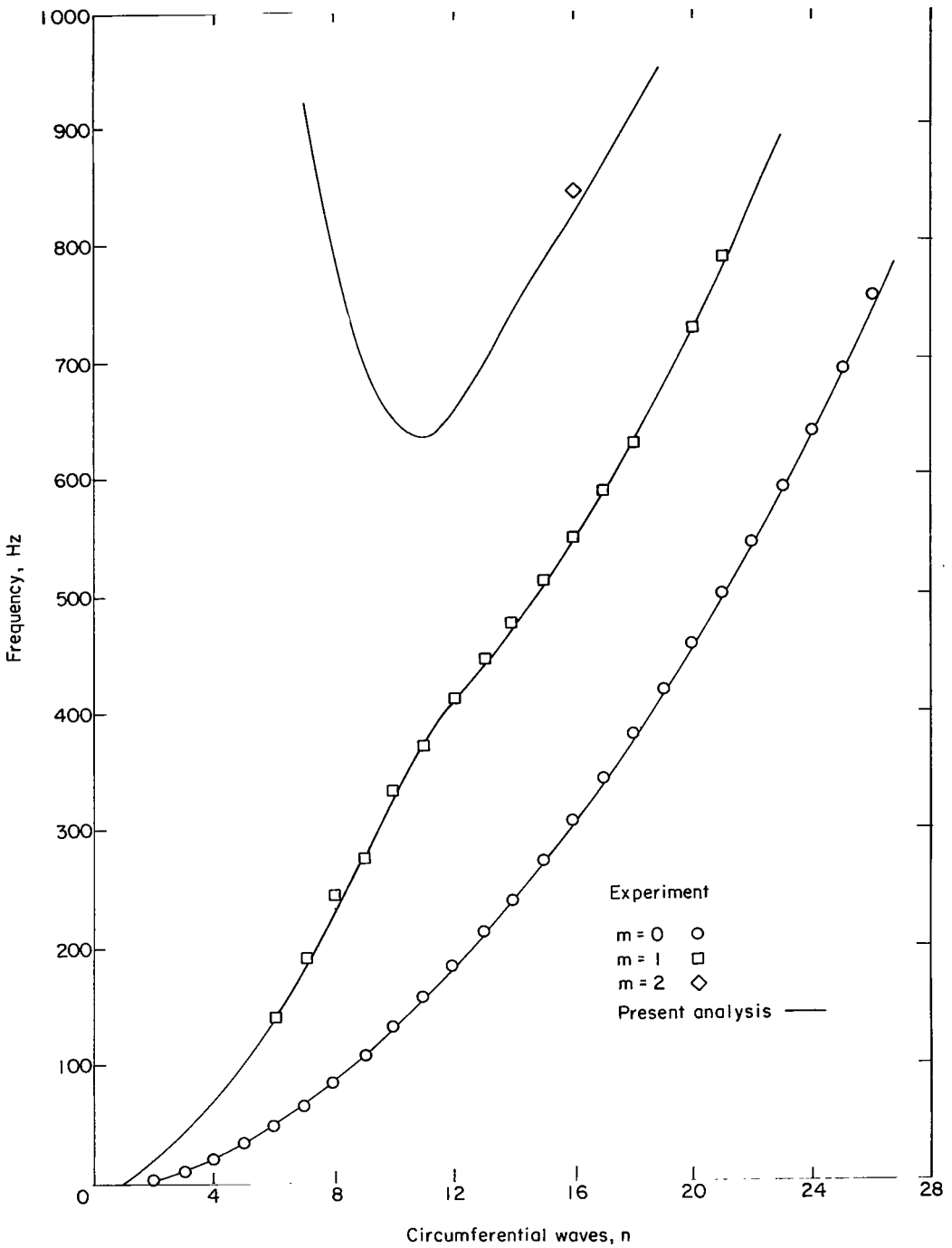

(d) 60.5^0 cone; $\frac{r_1}{r_2} = \frac{1}{2.25}$.

Figure 8.- Concluded.

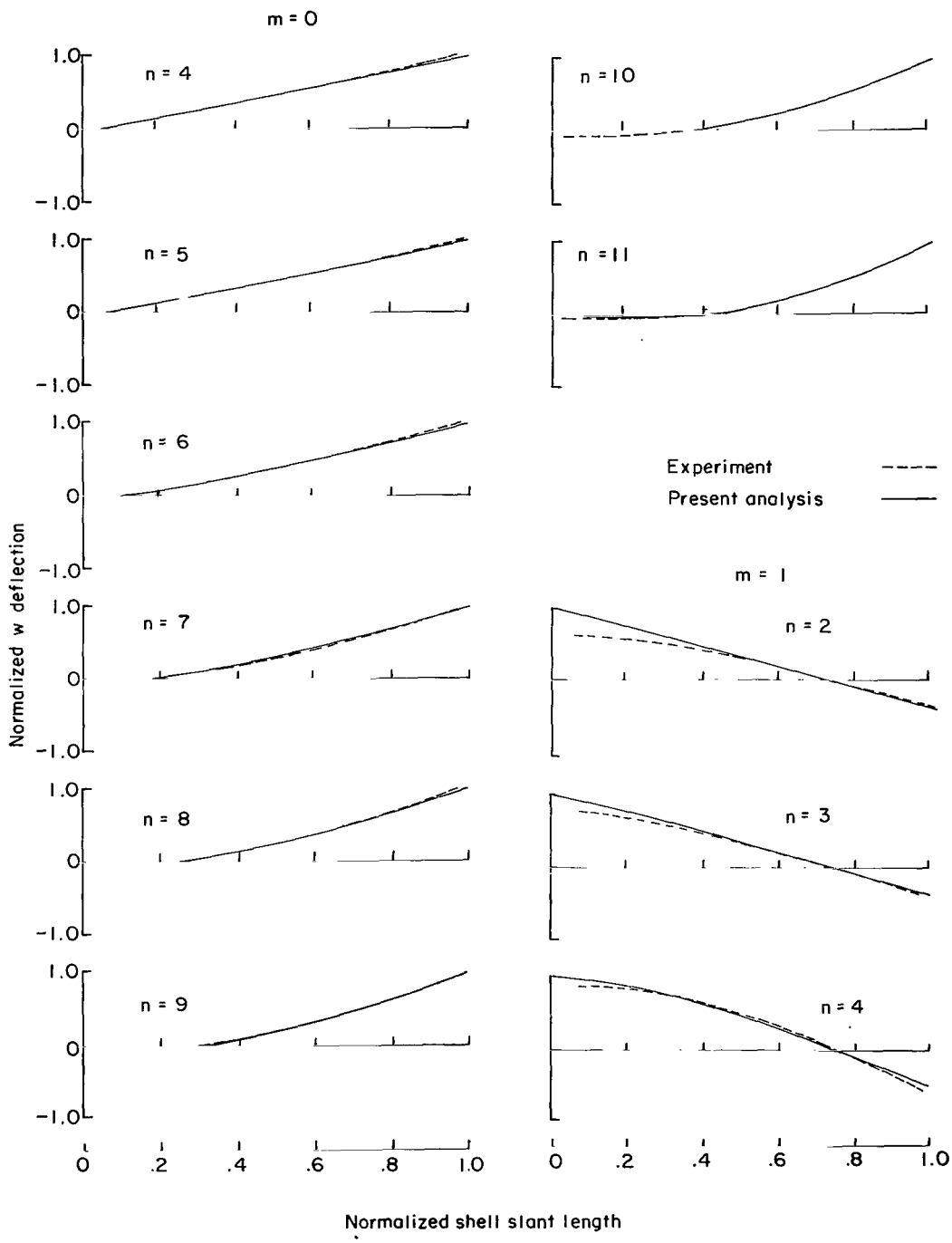

Figure 9.- Comparison of theoretical and experimental meridional mode shapes. Data source (1).

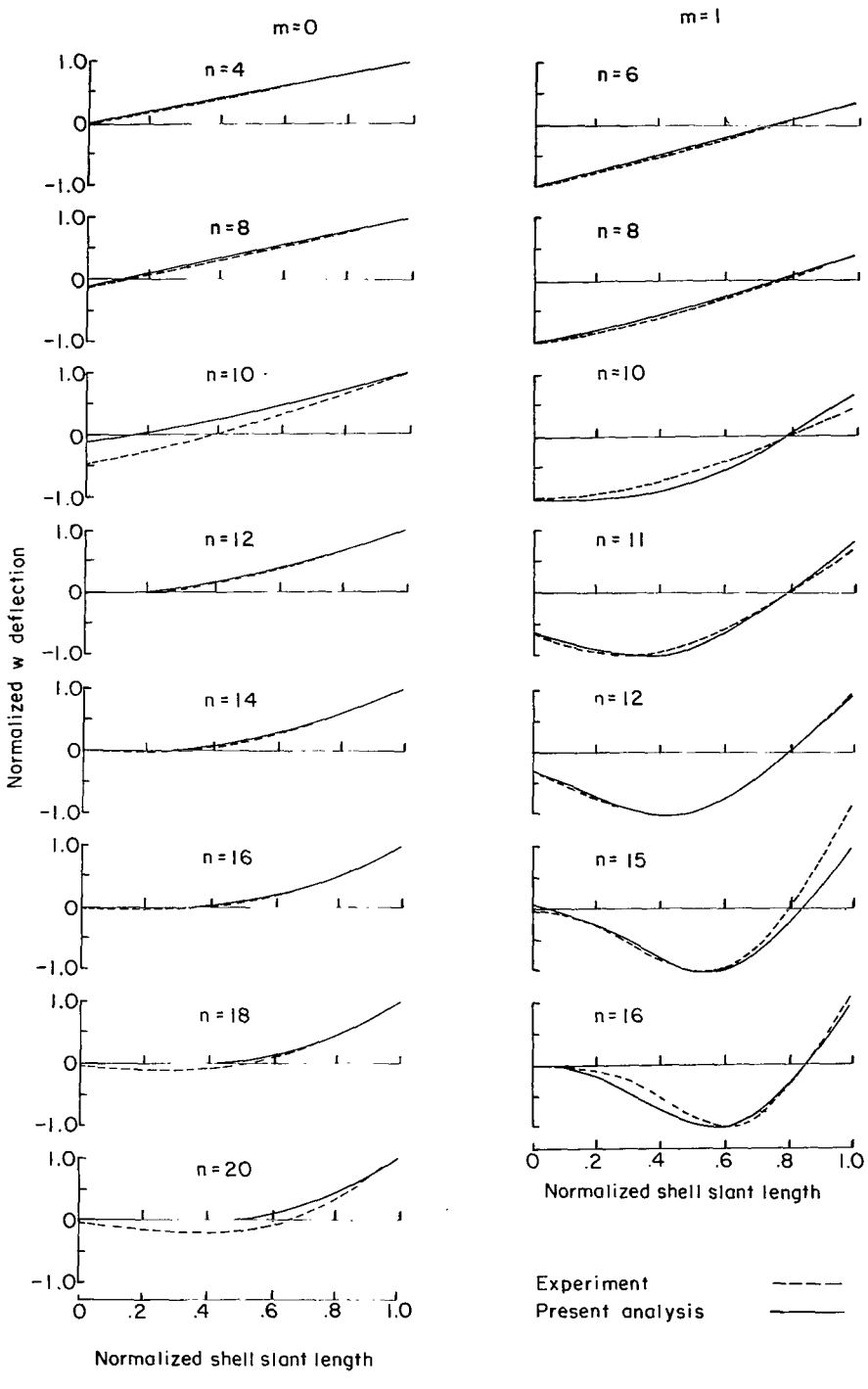

Figure 10.- Comparison of theoretical and experimental mode shapes. Data source (4).

NATIONAL AERONAUTICS AND SPACE ADMINISTRATION
WASHINGTON, D. C. 20546

OFFICIAL BUSINESS

FIRST CLASS MAIL

POSTAGE AND FEES PAID
NATIONAL AERONAUTICS AND
SPACE ADMINISTRATION

POSTMASTER: If Undeliverable (Section 158 Postal Manual) Do Not Return

"The aeronautical and space activities of the United States shall be conducted so as to contribute . . . to the expansion of human knowledge of phenomena in the atmosphere and space. The Administration shall provide for the widest practicable and appropriate dissemination of information concerning its activities and the results thereof."

—NATIONAL AERONAUTICS AND SPACE ACT OF 1958

NASA SCIENTIFIC AND TECHNICAL PUBLICATIONS

TECHNICAL REPORTS: Scientific and technical information considered important, complete, and a lasting contribution to existing knowledge.

TECHNICAL NOTES: Information less broad in scope but nevertheless of importance as a contribution to existing knowledge.

TECHNICAL MEMORANDUMS: Information receiving limited distribution because of preliminary data, security classification, or other reasons.

CONTRACTOR REPORTS: Scientific and technical information generated under a NASA contract or grant and considered an important contribution to existing knowledge.

TECHNICAL TRANSLATIONS: Information published in a foreign language considered to merit NASA distribution in English.

SPECIAL PUBLICATIONS: Information derived from or of value to NASA activities. Publications include conference proceedings, monographs, data compilations, handbooks, sourcebooks, and special bibliographies.

TECHNOLOGY UTILIZATION PUBLICATIONS: Information on technology used by NASA that may be of particular interest in commercial and other non-aerospace applications. Publications include Tech Briefs, Technology Utilization Reports and Notes, and Technology Surveys.

Details on the availability of these publications may be obtained from:

SCIENTIFIC AND TECHNICAL INFORMATION DIVISION

NATIONAL AERONAUTICS AND SPACE ADMINISTRATION

Washington, D.C. 20546